Obrabotka metallov –
Metal Working and Material Science

Journal homepage: http://journals.nstu.ru/obrabotka_metallov

The influence of structural state on the mechanical and tribological properties of Cu-Al-Si-Mn bronze

Andrey Filippov [a, *], Nikolay Shamarin [b], Sergei Tarasov [c], Natalya Semenchyuk [d]

Institute of Strenght Physics and Materials Sciences SB RAS, 2/4 per. Academicheskii, Tomsk, 634055, Russian Federation

[a] https://orcid.org/0000-0003-0487-8382, ✉ avf@ispms.ru; [b] https://orcid.org/0000-0002-4649-6465, ✉ shnn@ispms.ru;
[c] https://orcid.org/0000-0003-0702-7639, ✉ tsy@ispms.ru; [d] https://orcid.org/0000-0001-6547-7676, ✉ natali.t.v@ispms.ru

ARTICLE INFO

ABSTRACT

Introduction. Electron beam additive manufacturing (*EBAM*) is a promising method for producing new alloys with unique properties. At the same time, existing problems with obtaining a high-quality structure require a search for a technical solution that ensures grain refinement and the formation of a more homogeneous microstructure. For strain-hardened copper alloys, severe plastic deformation (*SPD*) methods are effective ways to control their structural state and mechanical properties. Currently, the effect of severe plastic deformation on the structure, mechanical, and tribological properties of *Cu-Al-Si-Mn* bronze, which is promising for industrial application, has not been studied. **The aim of this work** is to study the relationship between the structural state formed as a result of severe plastic deformation and the mechanical and tribological properties of *Cu-Al-Si-Mn* bronze samples. The paper studies samples of *Cu-Al-Si-Mn* bronze, made from bronze (*3% Si-1% Mn*) wires and commercially pure aluminum using multiwire electron beam additive manufacturing. For targeted changes in structure and properties, the resulting additively manufactured blanks were subjected to severe plastic deformation. Multi-axial forging and rolling were used as *SPD* methods, aimed at significant grain refinement and increased strength characteristics. The work uses such **research methods** as transmission electron microscopy (*TEM*) for a detailed analysis of the submicron structure after *SPD*, X-ray diffraction (*XRD*) to identify the phase composition of the alloy, tensile tests to determine key mechanical properties such as tensile strength, yield strength, and percentage of elongation, microhardness measurements to assess the hardening of samples using *Vickers* loads, confocal laser scanning microscopy (*CLSM*) for three-dimensional analysis of the surface topography and studying the morphology of worn surfaces, and dry sliding friction tests to assess the wear resistance of the material and the friction coefficient in the absence of lubrication under specified loads and sliding speeds. **Results and discussion.** Based on the data of transmission electron microscopy, it was found that the use of multi-axial forging and rolling led to significant changes in the structure of the material, as well as its phase composition. Based on the X-ray diffraction analysis, it was revealed that severe plastic deformation contributed to the deformation-induced dissolution of the **γ**- and **β**-phases. The results of tensile tests showed that the highest strength is achieved after intense plastic deformation by rolling, after multi-axial forging. *SPD* by multi-axial forging and subsequent rolling led to an increase in the microhardness of bronze. The results of tribological tests showed that *SPD* contributes to a decrease in the friction coefficient (*FC*) compared to the material in the printed state. Heat treatment of samples after *SPD* led to an increase in *FC* and an increase in fluctuations in its value. *SPD* by multi-axial forging and subsequent rolling contributes to a significant increase in the wear resistance of samples under dry sliding friction conditions. Low-temperature annealing after *SPD* leads to a decrease in the wear resistance of deformed samples. Thus, the use of *SPD* makes it possible to increase the strength and wear resistance of bronze samples of the *Cu-Al-Si-Mn* system.

Introduction

Bronzes are metal alloys that have a range of qualities making them essential for numerous uses, especially in corrosive environments and under sliding friction. The structural and phase states of bronzes dictate their mechanical, tribological, and corrosion properties, which are chosen based on the alloy's intended use and can be modified through suitable alloying. The key alloying elements for bronzes are aluminum, iron, nickel, tin, zinc, lead, manganese, and silicon, which are part of the composition of well-known bronze grades from the *Cu-Al*, *Cu-Mn*, *Cu-Zn*, *Cu-Pb*, *Cu-Si*, *Cu-Al-Fe*, *Cu-Ni-Al*, and *Cu-Al-Fe-Ni*

---

* Corresponding author
Filippov Andrey V., Ph.D. (Engineering), Head of Laboratory
Institute of Strenght Physics and Materials Sciences SB RAS,
2/4 per. Academicheskii,
634055, Tomsk, Russian Federation
Tel.: +7 999 178-13-40, **e-mail:** avf@ispms.ru

systems. The desired level of properties is attained not just by adjusting the alloying components but also through further thermal treatment and mechanical processing, which influences the material's physical and mechanical properties [1]. Even though a significant amount of work has already been accomplished in this field, ongoing exploratory research continues to be directed toward the creation of innovative structural and functional materials to meet contemporary industrial demands [1].

Although significant progress has been made in this field, ongoing exploratory research continues to focus on creating new structural and functional materials for contemporary industrial requirements.

The present phase of progress in material technologies is linked to the enhancement of additive techniques for creating items from robust materials that have excellent processability, adequate corrosion resistance, and wear resistance. To achieve an additive material with an adequate level of strength and functional characteristics, it is essential to identify a logical combination of printing parameters and filament formulation. The most crucial factor is the selection of the alloying element composition that will yield the required structure and phase constitution. Following this, the thermal treatment and mechanical processing modes for the printed material are established to achieve the intended functional characteristics.

Aluminum bronzes are noted for their excellent strength and formability under pressure. Incorporating silicon enhances ductility and improves resistance to corrosion and cyclic impact loads, all while preserving high strength. These properties can be further enhanced by adding manganese to the *Cu-Al-Si* system, which promotes increased strength, hardness, and corrosion resistance. Silicon and manganese enhance the stability of the ductile *FCC* α-phase formed from alloying elements in copper and inhibit the development of the brittle β-Cu_3Al phase. Nonetheless, high concentrations of these elements can also result in the formation of silicide particles and other reinforcement phases within the *Mn-Al* system. This is crucial for enhancing the mechanical characteristics of bronze through mechanical processes (forging, rolling, etc.). In industrial alloys of the *Cu-Al* system, with approximately 8–12 wt. % *Al*, the phases that exist in equilibrium at room temperature include the solid solution phase α-*Cu(Al)* and the intermetallic compounds β-Cu_3Al and $γ_2$-Cu_9Al_4. The latter is the product of the decomposition of high-temperature β-Cu_3Al into $γ_2$-Cu_9Al_4 and α-*Cu*. The development of $γ_2$-Cu_9Al_4 causes a reduction in the plasticity and corrosion resistance of bronze; thus, attempts are being made to remove it. One method to accomplish this could involve encouraging the diffusionless change from β to β′. The presence of β′-Cu_3Al greatly influences the mechanical characteristics by enhancing microhardness and strength [5, 6, 7].

In the *Cu-Si* system, the predominant phase is the solid solution α-*Cu(Si)*. A multiphase composition, comprising copper silicides, develops when the silicon content exceeds 5 wt.% [8]. The creation of copper silicides with higher silicon levels leads to enhanced strength and hardness in copper alloys [9].

The scenario is more intricate with the *Cu-Al-Si* system. The majority of the research on this system centers on analyzing the phase composition in areas with ele-vated aluminum levels [10–12], along with high silicon concentrations [13]. It has been previously noted that in such bronze, structures with *FCC*, *BCC*, and *HCP* crystal lattices, along with silicide particles, may develop [14]. The composition of phases is directly influenced by the amounts of aluminum and silicon, along with the temperature and the rate of solidification. This study suggests that a rise in aluminum content aids in creating a more multiphase structure. According to the modeling results [15], at temperatures of 500 °C and 700 °C in the *Cu-Al-Si* ternary system with approximately 10 at.% *Al* and about 3 at.% *Si*, the alloy appears to be multiphase. Nonetheless, this paper does not provide findings from structural studies that validate this information.

Aluminum bronzes typically exhibit a structure with large columnar grains or dendrites after casting. Similarly, in the three-dimensional printing process using electron beam additive manufacturing, bronzes based on copper-aluminum (*Cu-Al*), copper-silicon-manganese (*Cu-Si-Mn*), and copper-aluminum-manganese (*Cu-Al-Mn*) systems also develop a columnar grain structure in the samples [16–18]. These grains are undesirable, hindering the material's strength and ductility. Therefore, a critical challenge for current researchers is to devise methods for controlling the microstructure of bronze alloys – through techniques like thermomechanical processing or alloying — to ensure improvements in their strength, wear resistance, and fatigue life.

Bronzes containing aluminum, silicon, and manganese are considered strain-hardening alloys. Applying severe plastic deformation (*SPD*) methods is a practical approach to intentionally modify their structural-phase state and, thereby, their mechanical properties. These methods encompass: forging, rolling, equal-channel angular pressing, high-pressure torsion, and surface plastic deformation [19, 20].

Currently, the impact of *SPD* on the structural, mechanical, and tribological characteristics of the *Cu-Al-Si-Mn* bronze system, a material with considerable potential for industrial use, remains unexplored. This is particularly the case for materials fabricated via additive manufacturing techniques.

In light of the foregoing review, the inherent promise of the material, and the identified deficiencies in existing studies, the ***objective of this research*** was established: to explore the correlations between the diverse structural states and the properties of the *Cu-Al-Si-Mn* copper alloy.

To realize this objective, the following experimental ***tasks*** were undertaken:

– to characterize the structure and phase composition of samples in the as-printed condition and following the application of intense plastic deformation techniques;

– to evaluate mechanical properties, specifically tensile strength and microhardness, for samples exhibiting various structural states;

– to analyze the tribological behavior of the samples;

– to examine the morphology of the wear track surfaces.

Methods

To investigate the influence of structural states on the properties of *Cu-Al-Si-Mn* bronze, samples in the form of prismatic blocks ($20\times20\times40$ mm³) were fabricated using electron beam additive manufacturing. Printing was performed by simultaneously feeding two wires: *Cu-3 Si-1 Mn* (*BrKMts 3-1*) and commercially pure aluminum, in a ratio of 90 % bronze to 10 % aluminum [21]. The chemical composition of the samples was 93.8 wt.% *Cu*, 2.5 wt.% *Al*, 2.8 wt.% *Si*, 0.9 wt.% *Mn*. The printed blocks were subjected to severe plastic deformation (*SPD*) by means of multi-directional forging and rolling. In addition, the samples were also subjected to low-temperature heat treatment after *SPD*. The designations of the investigated samples and the processing parameters are listed in Table.

Designation of samples and methods for forming their structure

Sample designation	Method of forming a structural state
1	Electron beam additive manufacturing
2	Multi-axial forging along three geometric axes until 40% plastic deformation is achieved in each direction
3	Rolling after multi-axial forging until 50% plastic deformation is achieved
4	Low-temperature annealing (30 min. at 400°C) after multi-axial forging with rapid cooling in water
5	Low-temperature annealing (30 min. at 400°C) after rolling with rapid cooling in water

Flat tension test specimens were cut from the obtained samples using an electrical discharge machine for mechanical testing on a *Testsystem UTS-110M* testing machine. The tensile speed was 1 mm/min. Samples in the form of plates were additionally cut for conducting X-ray diffraction analysis on a *Shimadzu XRD-7000* diffractometer. Microhardness measurements were performed using a *Tochline-TBM* microhardness tester with a load of 100 N. The fine structure of the samples was investigated by transmission electron microscopy on a *JEOL JEM-2100* microscope.

Tribological tests were conducted at a fixed sliding speed of 0.1 m/s and a normal load of 20 N under dry sliding friction conditions using a pin-on-disk scheme. Disks were cut from bronzes with different structural states. Counterbodies were made of ball-bearing steel (*1 C-1.5 Cr*). *Tescan MIRA 3 LMU* and *Olympus OLS-4100* microscopes were used to investigate the surface condition of the samples after friction

using scanning electron microscopy and laser scanning microscopy, respectively. Energy-dispersive X-ray spectroscopy (*EDS*) was performed to identify the features of the sample condition after friction.

Results and Discussion

Based on previously obtained results [21] from metallographic studies, it was established that the structure of the printed bronze consists of α-*Cu(Al)* solid solution grains with a size of approximately 75 μm, interspersed with layers of a secondary phase. Upon examination of the fine structure using transmission electron microscopy, it was revealed that the printed bronze (Sample 1) exhibits laths representing α/β eutectoid lamellae, in which the decomposition β→$γ_2$+ α has occurred (Fig. 1, *a*). The high dislocation density and two overlapping systems of deformation twins (Fig. 1, *b*) are a result of multi-directional forging (Sample 2). Rolling (Sample 3) creates a high dislocation density and deformation twins within the material (Fig. 1, *c*). Primary systems of deformation twins can be disrupted due to the high degree of deformation and replaced by secondary ones, which are significantly smaller than those formed during the multi-directional forging stage. In Sample 4 (Fig. 1, *d*), one system of deformation twins predominates, remaining intact even after annealing, indicating their sufficiently high stability with respect to heating. In Sample 5 (Fig. 1, *e*), stacking faults, recrystallized submicron grains, and annealing microtwins were formed in the material. These structural changes indicate that the high degree of deformation promoted recrystallization of grains even during annealing below the recrystallization temperature.

X-ray diffraction analysis revealed the influence of the *SPD* method and subsequent heat treatment on the phase composition of the printed bronze. The X-ray diffraction patterns clearly show intense reflections of the α-*Cu(Al)* phase, with the (111) peak being the highest, indirectly indicating the absence of a growth texture (Fig. 2, *a*). Upon detailed examination, reflections of $γ_2$-Cu_9Al_4 were also identified, which are only found in samples of the as-printed bronze (Sample 1, Figs. 2, *c*, *d*) and samples after multi-directional
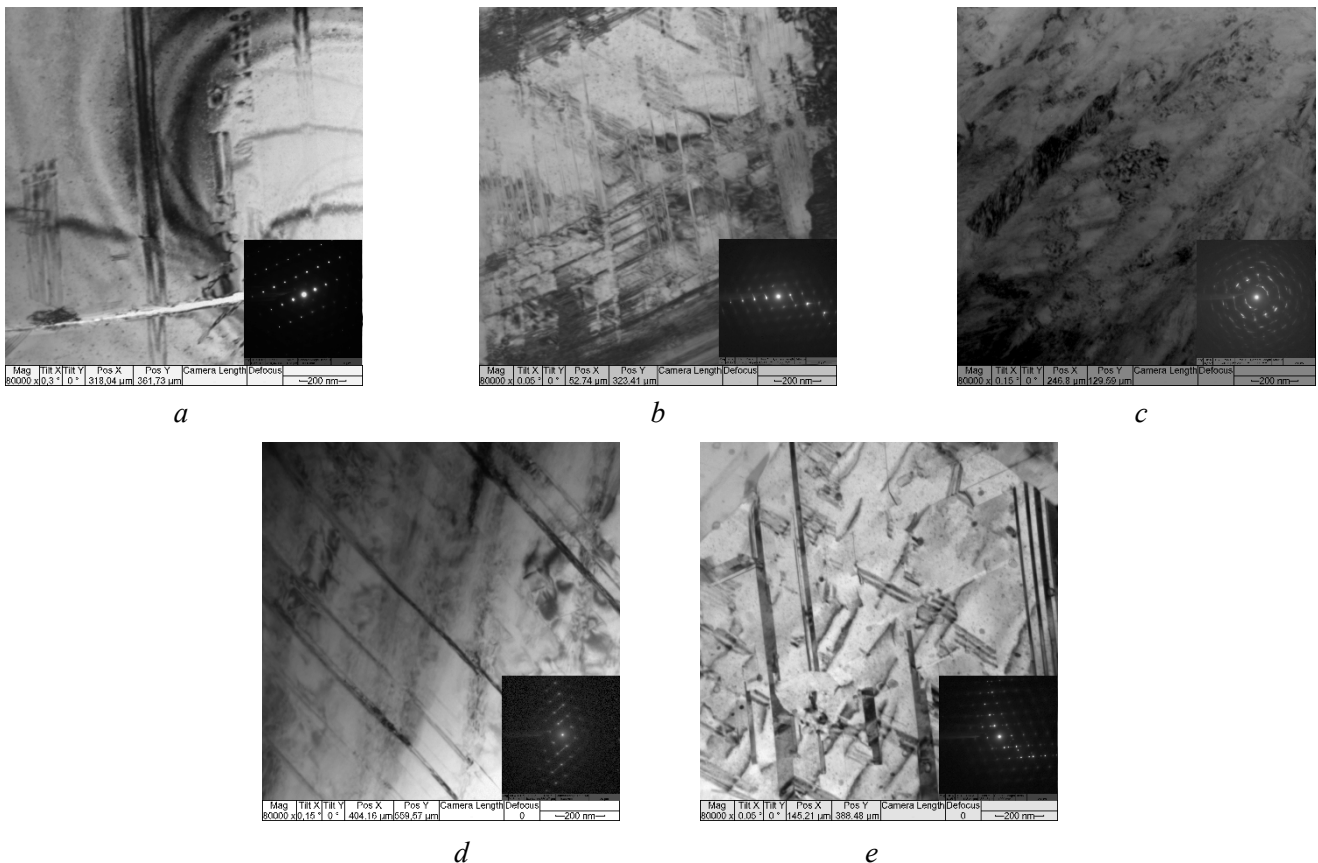

a　　　　　　　　　　*b*　　　　　　　　　　*c*

d　　　　　　　　　　*e*

Fig. 1. TEM images of the typical microstructure of *Cu-Al-Si-Mn* bronze samples. Sample 1 (*a*), sample 2 (*b*), sample 3 (*c*), sample 4 (*d*) and sample 5 (*e*)
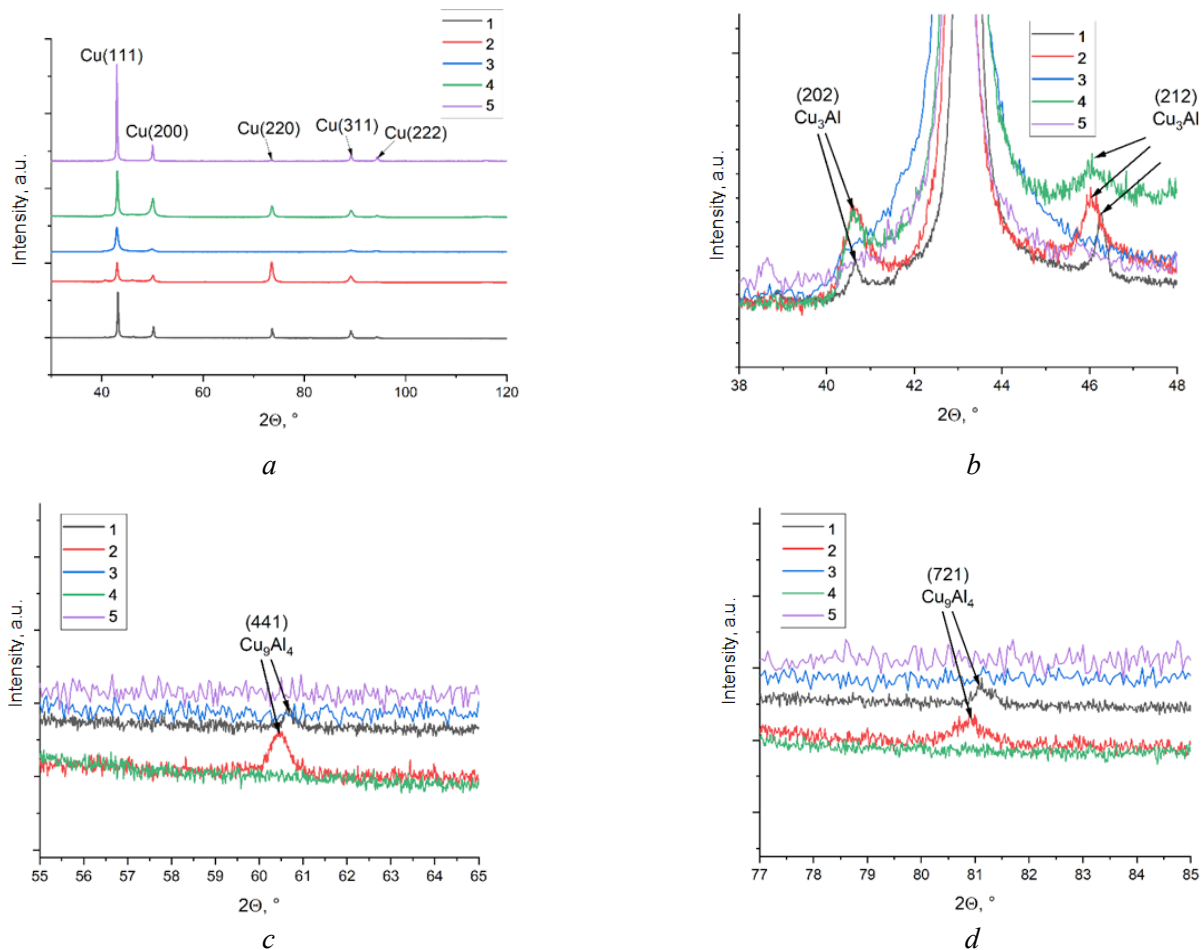
Fig. 2. X-ray diffraction (*XRD*) patterns of *Cu-Al-Si-Mn* bronze samples

forging (<u>Sample 2</u>, Figs. 2, *c*, *d*). The intensity of the reflections from this phase increased after multi-directional forging, presumably due to the formation of γ_2-Cu_9Al_4 during plastic deformation within the *Cu-Al* system. It is known that γ_2-Cu_9Al_4 is formed during mechanical alloying and friction stir processing and decomposes into its components when heated above 180 °C [22]. Therefore, either intermediate annealing before rolling or complete annealing at 400 °C can completely eliminate this phase.

In addition, reflections of the β-Cu_3Al phase are observed, which are found in samples of the as-printed bronze (<u>Sample 1</u>, Figs. 2, *c*, *d*), samples after multi-directional forging (<u>Sample 2</u>, Figs. 2, *c*, *d*), and heat-treated samples after multi-directional forging (<u>Sample 4</u>, Figs. 2, *c*, *d*).

One of the key factors affecting the phase composition of samples after *SPD* is the mechanism of deformation-induced dissolution of intermetallic phases [23]. As a result of *SPD*, particles of secondary phases dissolve, are fragmented, and refined under the influence of high stresses and a dislocation density close to the theoretical limit [24]. The possibility of precipitation of finely dispersed intermetallic particles is also not excluded, which is also a consequence of *SPD* and leads to additional strengthening of the alloy.

The modification of the material's structure through severe plastic deformation (*SPD*), followed by subsequent heat treatment, resulted in changes to the mechanical properties of the bronze, in comparison to the as-printed condition. The conducted investigations clearly demonstrate that the sequential application of *SPD* methods — namely, multi-directional forging and rolling — causes a substantial increase in the tensile strength of the bronze compared to the initial state obtained by the electron beam additive manufacturing method (Fig. 3, *a*).

In particular, the use of multi-directional forging provided a significant strength increase of 179 MPa, while the rolling process led to an even more pronounced enhancement of mechanical properties, increasing the tensile strength by 515 MPa.

Following heat treatment via annealing, conducted at a temperature of 400 °C, a further strengthening effect was demonstrated for both types of deformed samples. Notably, for samples that had undergone multi-directional forging, annealing contributed to a further increase in tensile strength by 30 MPa. Regarding the samples after rolling, annealing at the same temperature resulted in a more substantial additional increase in strength, amounting to 43 MPa.

The performed analysis also revealed that *SPD* induces a significant increase in the yield strength of the bronze, relative to the characteristics of the samples formed after additive manufacturing. Multi-directional forging led to a substantial increase in yield strength (by 359 MPa), whereas the application of rolling produced an even more significant increase – 725 MPa

Subsequent heat treatment via annealing, also demonstrated a positive influence on this parameter for all types of samples considered after *SPD*. In particular, for samples pre-processed by multi-directional forging, annealing contributed to a further increase in yield strength by 16 MPa. In the case of samples subjected to rolling, a similar annealing process resulted in a greater additional increase in yield strength, which amounted to 26 MPa.

The application of multi-directional forging and rolling led to a reduction in the relative elongation of the bronze samples by 2.6 and 4.5 times, respectively, compared to the as-printed sample (Fig. 3, *b*). Annealing at 400 °C resulted in a minor increase in relative elongation of 1.1 % for the sample after multi-directional forging and 1.8 % for the sample after rolling.
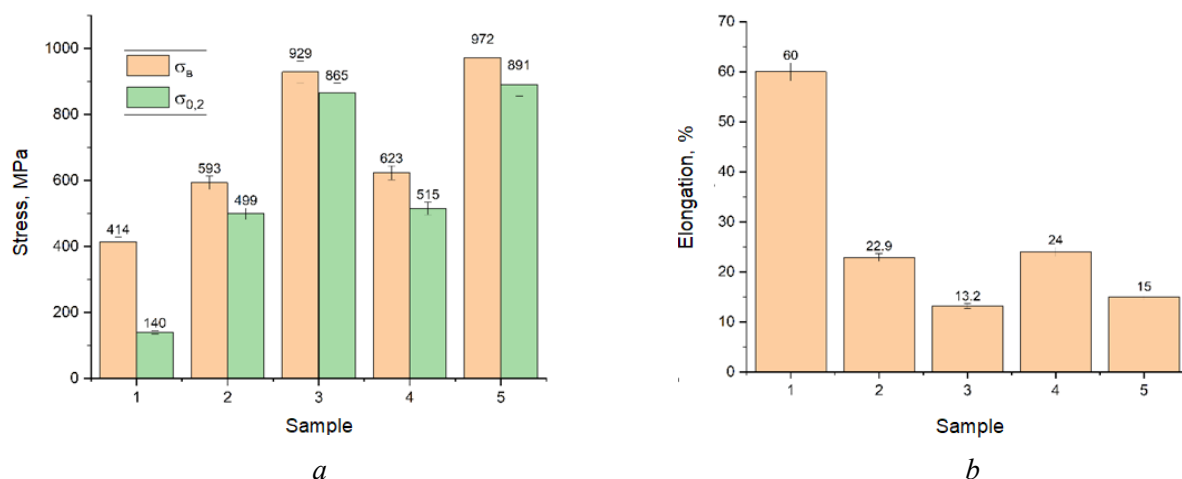

Fig. 3. Mechanical properties of *Cu-Al-Si-Mn* bronze samples

Based on the experimental data, it was established that *SPD* significantly affects the strength and ductility of the printed *Cu-Al-Si-Mn* bronze samples. An increase in strength and a decrease in ductility are expected for an alloy with an *FCC* lattice, due to strain hardening mechanisms and structural refinement. Annealing has a minimal impact on the strength of the post-SPD samples, while their ductility improves by approximately 5–13.6 % compared to the deformed state. This is due to the influence on the structure and phase composition of the samples. On the one hand, annealing led to partial recrystallization of the structure and a reduction in the number of crystal lattice defects. On the other hand, the sizes of the structural elements remained at the submicron level. As a result, an increase in ductility and the retention of the material's strength were achieved. The small increase in strength after annealing is associated with the cooperative contribution from grain boundary and dislocation strengthening mechanisms in the *FCC* alloy and has been previously noted for alloys with an ultrafine-grained structure [25–29]. In addition, the contribution to solid solution strengthening comes from the deformation-induced dissolution of secondary phase particles [30], as well as the possible precipitation of dispersed phases from the solution as a result of aging.

Severe plastic deformation (*SPD*) through multi-directional forging followed by rolling increased the microhardness of the bronze by 46% and 80%, respectively, compared to the as-printed samples (Fig. 4). Annealing the multi-directionally forged sample at 400°C increased the microhardness from 2.05 GPa to

2.37 GPa. Based on the microstructural data and phase composition, the increased hardness is likely due to the dissolution of the primary β-phase and the precipitation of secondary coherent phases within the grain volume. Annealing the rolled sample at 400°C decreased the microhardness from 2.52 GPa to 2.25 GPa. As annealing did not alter the phase composition of the rolled sample, the change in microhardness is attributed solely to structural modifications within the material.

During the tribological tests, the change in the coefficient of friction (*CoF*) over time was recorded (Fig. 5, *a*), from which the average value was calculated (Fig. 5, *b*). When the printed bronze sample (Sample 1) was subjected to friction, the *CoF* remained relatively constant throughout the test at 0.245, with the amplitude of fluctuations not exceeding 0.02. In addition to changing the mechanical properties, multi-directional forging also affected the tribological properties of the investigated bronze. At the start of the test, the *CoF* for Sample 2 was 0.2, but then decreased to 0.14 within the first 300 seconds. Then the *CoF* gradually increased to 0.172, and its short-term fluctuations did not exceed 0.05. After rolling (Sample 3), the *CoF* changed insignificantly; its average value was 0.189, and short-term fluctuations were 0.03. Heat treatment of the sample after multi-directional forging led to an increase in the average *CoF* to 0.18, and short-term fluctuations to 0.05 (Fig. 5, *a*, Sample 4). During friction, the *CoF* monotonically increased from the beginning to the end of the test. Heat treatment of the sample after rolling led to an increase in the average *CoF* to 0.226, and short-term fluctuations to 0.05 (Fig. 5, *a*, Sample 5). The change in *CoF* during friction was not monotonic. At the initial stage, the *CoF* increased, but then decreased approximately in the second half of the test.

Fluctuations in the coefficient of friction reflect dynamic alterations during the sliding friction process. The greater their amplitude, the more unstable the friction process becomes, which may reflect a change in the conditions of contact interaction between the steel ball and the bronze. Based on the obtained results, it can be noted that *SPD* contributes to a reduction in the *CoF* compared to the as-printed material. Heat treatment of the samples after *SPD* led to an increase in the *CoF* and an increase in the amplitude of its fluctuations.

Based on the analysis of optical image data, characteristic regions reflecting the condition of the wear track surface on the bronze samples were identified (Fig. 6). After friction of the as-printed bronze, fine microgrooves formed on the track, oriented along the direction of the friction force, along with dark areas
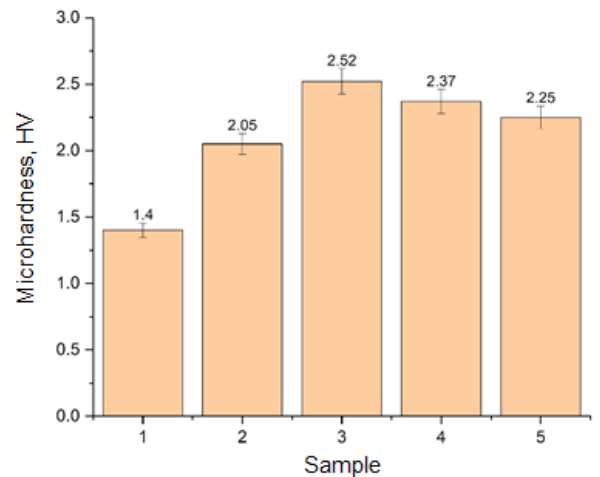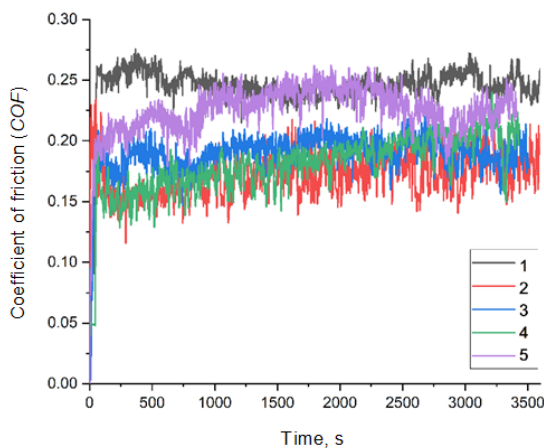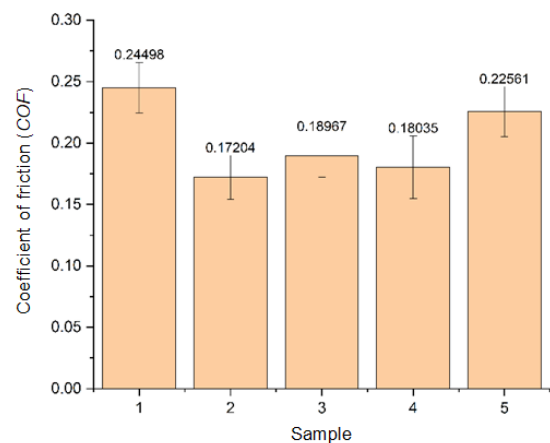
Fig. 4. Microhardness of *Cu-Al-Si-Mn* bronze samples

a　　　　　　　　　　*b*

Fig. 5. Coefficients of friction as a function of time during sliding tests (*a*) and their average values (*b*)

containing oxidized material (Fig. 6, *a*). Signs of plastically displaced material are visible at the edges of the track, indicating substantial plastic deformation of the material. Following friction of the bronze sample with the structure produced by multi-directional forging (Fig. 6, *b*), fragments of detached wear particles are observed on the surface, in addition to microgrooves and extended regions of oxidized material. Rolling significantly influenced the post-friction condition of the material (Fig. 6, *c*). The resulting image reveals that the wear track consists of microgrooves without noticeable oxidation or wear debris. After annealing the multi-directionally forged sample (Fig. 6, *d*), the microgrooves are preserved and become more pronounced; the traces of oxidation approximately coincide with those observed on the deformed Sample 2. Concurrently, individual wear particles are absent. Annealing the rolled sample (Fig. 6, *e*) had a minimal effect on the morphology of the wear track surface; only a slight increase in its width was observed, suggesting an increase in the wear volume.
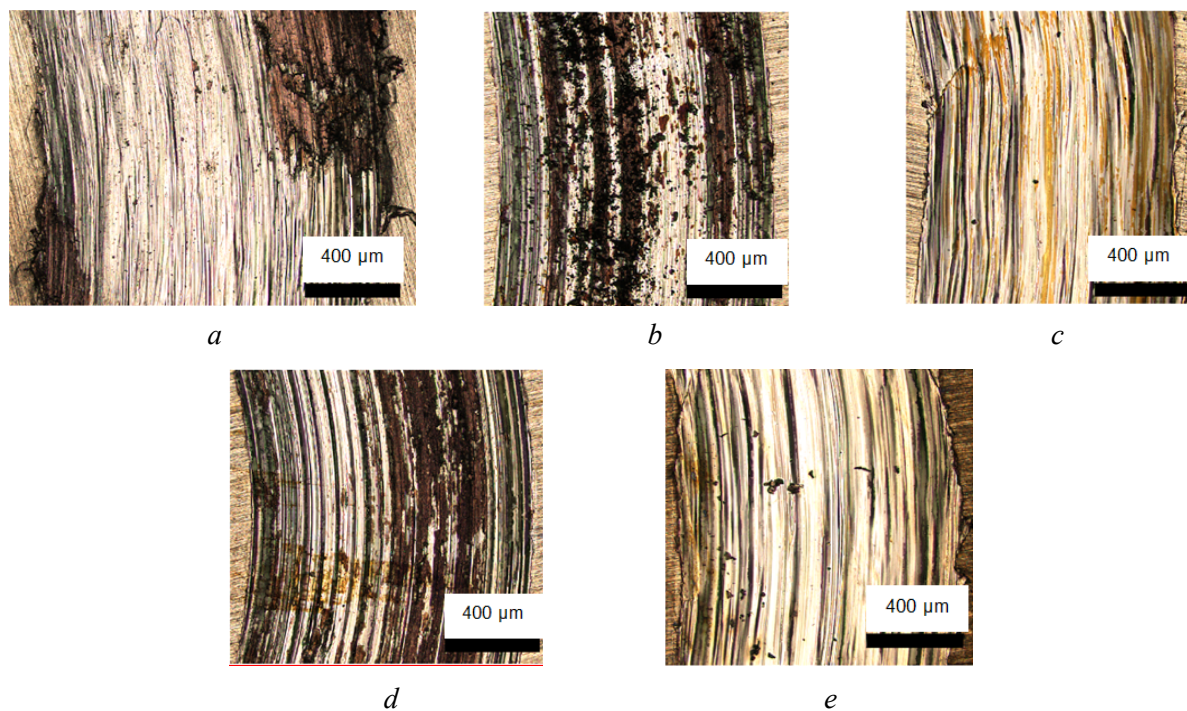

a *b* *c*

d *e*

Fig. 6. Optical images of the wear track surfaces of *Cu-Al-Si-Mn* bronze samples. Sample 1 (*a*),
sample 2 (*b*), sample 3 (*c*), sample 4 (*d*) and sample 5 (*e*)

Annealing promotes increased material plasticity; therefore, the amount of wear particles on the heat-treated samples after *SPD* by multi-directional forging decreased. This is attributed to a reduced likelihood of fracture of the ductile bronze material due to deformation induced by the steel counterbody.

Following the tribological tests, the surface condition of the steel balls was also investigated (Fig. 7). Signs of adhesive material transfer were observed on the surfaces of all the balls, a characteristic feature of bronze-steel friction pairs [31]. Bronze particles detaching during sliding friction adhered to the surface of the steel counterbody due to adhesive bonds. This process results in the formation of a protective layer, acting as a third body between the sample and the counterbody. The state of this layer is dependent on the wear characteristics of the softer material – the bronze. Previous results indicated that the wear of as-printed bronze results in the formation of microgrooves on its surface accompanied by minor oxidation. Correspondingly, grooves and minor areas with oxidized material are also observed on the surface of the ball (Fig. 7, *a*). Increased oxidation during friction of bronze Sample 2 and Sample 4 (following multi-directional forging and subsequent annealing) is reflected in the formation of an adherent layer on the counterbody's surface. Instead of microgrooves, the formation of a mechanical mixture of non-uniform thickness, composed of bronze and oxidized material, is observed (Fig. 7, *b*, *d*).
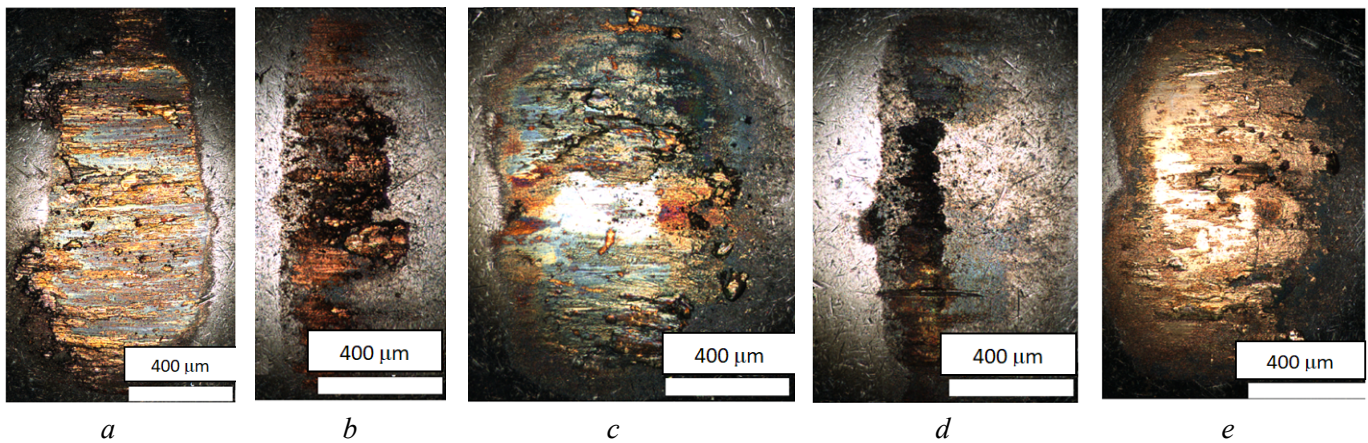
Fig. 7. Optical images of the steel ball surfaces after sliding against *Cu-Al-Si-Mn* bronze samples. Sample 1 (*a*), sample 2 (*b*), sample 3 (*c*), sample 4 (*d*) and sample 5 (*e*)

Following friction of <u>Sample 3</u> and <u>Sample 5</u> (Fig. 7 *c, d*), a noticeable layer of bronze, transferred from the wear track, forms on the surface of the balls. Its formation is attributed to a reduction in the oxidation of the copper alloy surface during sliding friction in the examined structural states, which also leads to less pronounced mechanical removal of material from the ball surfaces.

To provide a more detailed assessment of the wear track surface condition, energy-dispersive X-ray spectroscopy (*EDS*) analysis was performed (Figs. 8, 9). As a result of friction, dark layers of material formed, unevenly covering the worn surface of the *Cu-Al-Si-Mn* alloy samples. *EDS* analysis revealed that these layers contained an increased concentration of oxygen (Fig. 9). Therefore, these layers consist of a mechanical mixture of bronze and wear particles, which underwent oxidation due to thermomechanical
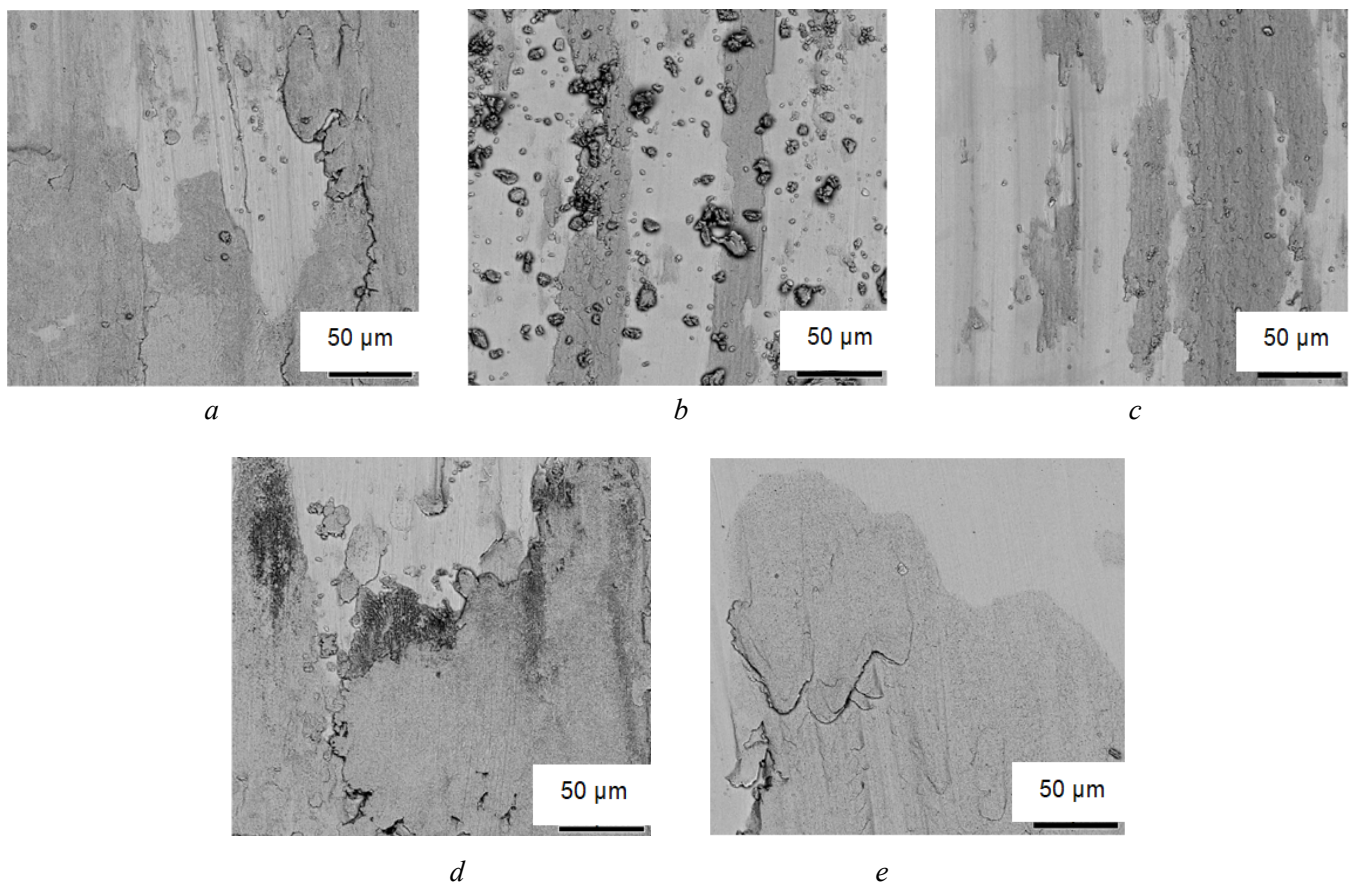

Fig. 8. SEM images of the wear track surfaces of *Cu-Al-Si-Mn* bronze. Sample 1 (*a*), sample 2 (*b*), sample 3 (*c*), sample 4 (*d*) and sample 5 (*e*)
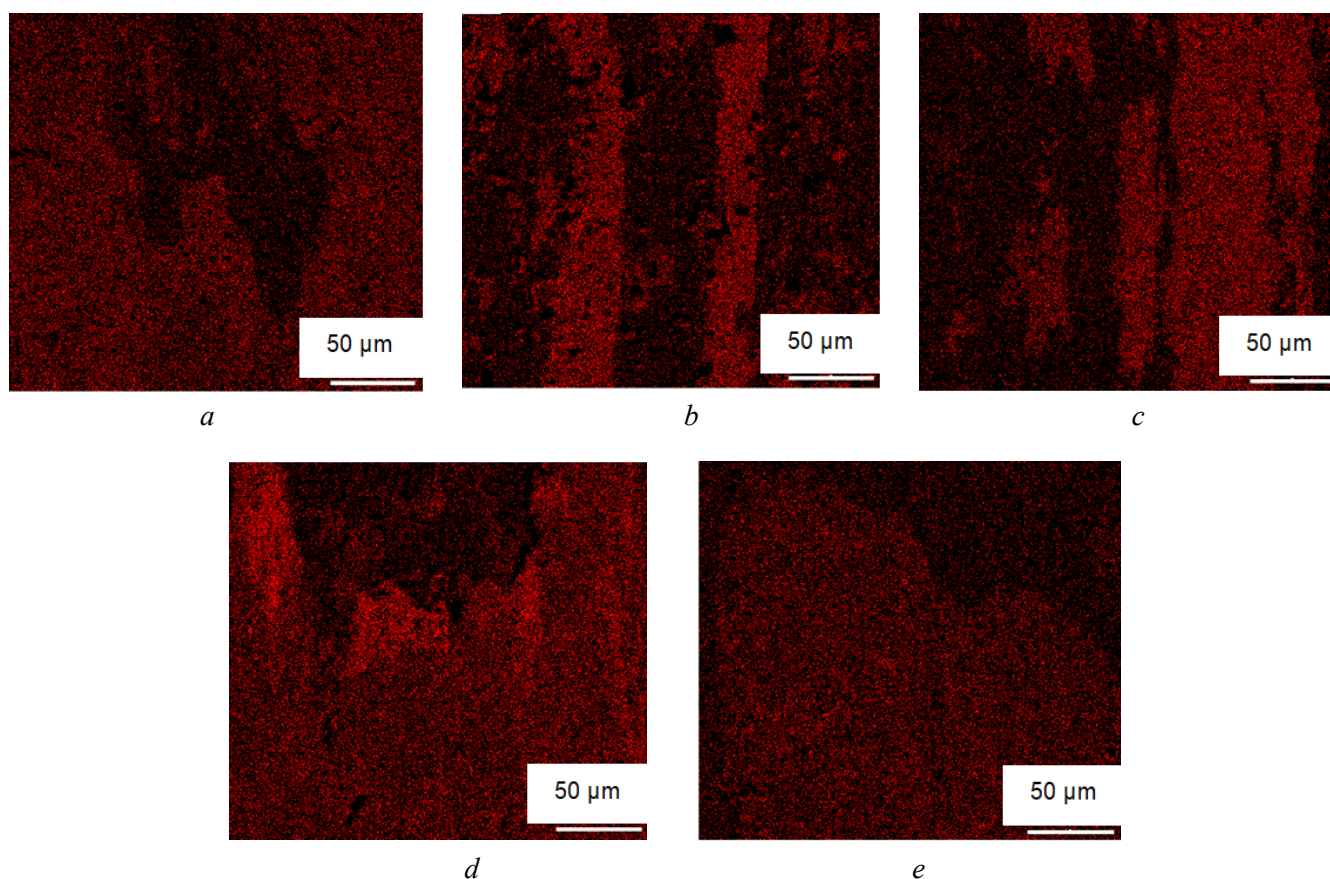
Fig. 9. Elemental mapping of oxygen on the wear track surfaces of *Cu-Al-Si-Mn* bronze. Sample 1 (*a*), sample 2 (*b*), sample 3 (*c*), sample 4 (*d*) and sample 5 (*e*)

action during sliding friction. During friction, these layers were disrupted by repeated mechanical action from the counterbody.

Three-dimensional surface scanning provided detailed data on the morphology of the wear track cross-sections, as shown in Fig. 10. The profile shape of each track closely mirrored the spherical configuration of the steel balls used, without any noticeable deviations. Furthermore, the track profiles clearly visualized characteristic surface microroughness formed during frictional interaction and subsequent wear of the material.

Quantification of wear, achieved through accurate determination of the cross-sectional area of the obtained profiles, revealed a significant disparity in the wear resistance of the samples. Specifically, printed
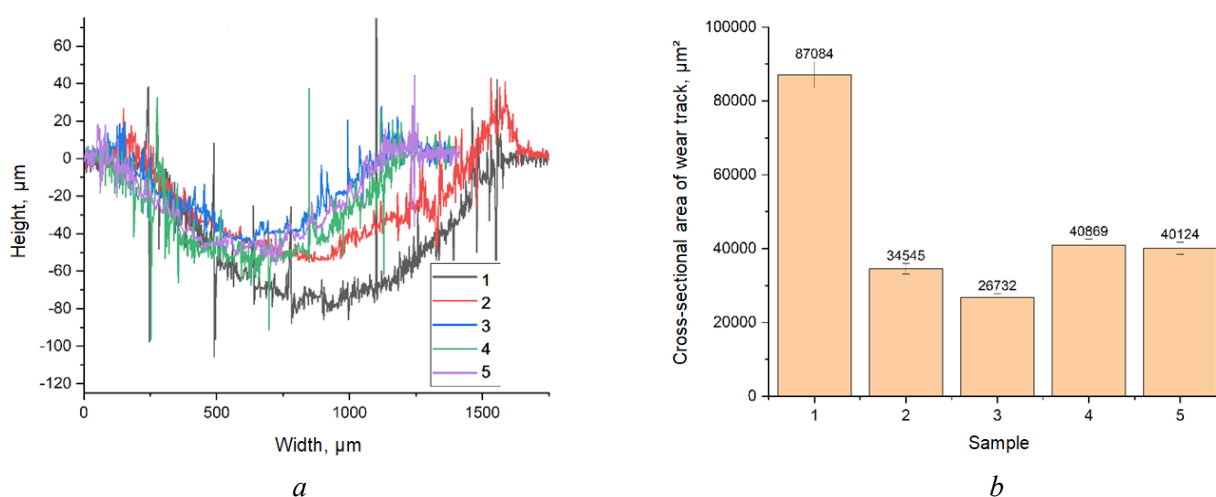

Fig. 10. Cross-sectional profiles (*a*) and areas (*b*) of the wear tracks of *Cu-Al-Si-Mn* bronze

sample 1 (Fig. 10) exhibited the lowest wear resistance, supported by the highest wear area value of 87,084 µm², significantly exceeding the respective values of the other examined samples. The wear on the sample after multi-side forging (Fig. 10, sample 2) was notably lower, measuring 34,545 µm². The sample's wear after rolling (Fig. 10, sample 3) was the lowest at 26,732 µm². Following heat treatment after multi-side forging, the wear of the specimen (Fig. 10, sample 4) increased to 40,869 µm². Following heat treatment after rolling, the wear of the sample (Fig. 10, sample 5) increased to 40,124 µm². These experimental data confirm that incremental plastic deformation (*IPD*) results in reduced bronze wear compared to the printed condition. Heat treatment, in turn, increased the wear of samples relative to their deformed state.

Conclusion

This study investigated the effect of severe plastic deformation (*SPD*) on the structural state, mechanical properties, and tribological performance of a *Cu-Al-Si-Mn* copper alloy fabricated by electron beam additive manufacturing. The experimental results established a correlation between the microstructure, tensile mechanical properties, and tribological behavior of the bronze alloy under unlubricated sliding friction.

1. *SPD* via multi-side forging and rolling resulted in a high density of dislocations and deformation twins within the material.

2. Annealing at 400 °C following multi-side forging led to partial recrystallization of the material; however, a system of deformation twins remained, demonstrating considerable structural stability. Low-temperature annealing at 400 °C after rolling resulted in the development of stacking faults, recrystallized submicron grains, and annealing micro-twins within the material.

3. X-ray diffraction analysis indicated that rolling and annealing induced deformation dissolution of secondary phases (β- and γ-phases), resulting in the *Cu-Al-Si-Mn* alloy becoming a single-phase consisting of the α-phase of face-centered cubic (*FCC*) copper.

4. Multi-side forging and rolling enhanced the tensile strength of the bronze alloy by factors of 1.43 and 2.24, respectively, while reducing its relative elongation by factors of 2.6 and 4.5 compared to the as-printed condition.

5. Annealing had a minimal impact on the strength of the post-*SPD* samples, whereas their ductility increased by approximately 5–13.6% relative to the deformed condition.

6. *SPD* via multi-side forging followed by rolling increased the microhardness of the bronze by 46% and 80%, respectively, compared to the as-printed samples. Annealing the sample at 400 °C after multi-side forging led to a 15.6% increase in microhardness. Annealing the sample at 400 °C after rolling resulted in a 12% decrease in microhardness.

7. Multi-side forging and rolling reduced wear by factors of 2.5 and 3.3, respectively, compared to the alloy in its as-printed state. Annealing increased the wear of the alloy by a factor of 1.5.

8. Based on these findings, a processing route involving a combination of multi-side forging, followed by rolling and low-temperature annealing, is proposed to enhance the mechanical and tribological properties of the *Cu-Al-Si-Mn* copper alloy. These experimental results provide valuable insights for developing practical strategies aimed at significantly improving the strength properties and wear resistance of bronzes in the *Cu-Al-Si-Mn* system, fabricated using electron beam additive manufacturing.

References

1. Osintsev O.E., Fedorov V.N. *Med' i mednye splavy: otechestvennye i zarubezhnye marki* [Copper and copper alloys. domestic and foreign brands]. 2nd ed., rev. Moscow, Innovatsionnoe mashinostroenie Publ., 2016. 360 p. ISBN 978-5-9907638-3-8.

2. Kolubaev E.A., Rubtsov V.E., Chumaevsky A.V., Astafurova E.G. Micro-, Meso- and macrostructural design of bulk metallic and polymetallic mate-rials by wire-feed electron-beam additive manufacturing. *Physical Mesomechanics*, 2022, vol. 25 (6), pp. 479–491. DOI: 10.1134/S1029959922060017.

3. Qu S., An X.H., Yang H.J., Huang C.X., Yang G., Zang Q.S., Wang Z.G., Wu S.D., Zhang Z.F. Microstructural evolution and mechanical properties of Cu-Al alloys subjected to equal channel angular pressing. *Acta Materialia*, 2009, vol. 57 (5), pp. 1586–1601. DOI: 10.1016/j.actamat.2008.12.002.

4. Massalski T.B. The Al-Cu (Aluminum-Copper) system. *Bulletin of Alloy Phase Diagrams*, 1980, vol. 1, pp. 27–33. DOI: 10.1007/BF02883281.

5. Kroupa A., Zobač O., Richter K.W. The thermodynamic reassessment of the binary Al-Cu system. *Journal of Materials Science*, 2021, vol. 56, pp. 3430–3443. DOI: 10.1007/s10853-020-05423-7.

6. Zobac O., Kroupa A., Zemanova A., Richter K.W. Experimental description of the Al-Cu binary phase diagram. *Metallurgical and Materials Transactions A*, 2019, vol. 50, pp. 3805–3815. DOI: 10.1007/s11661-019-05286-x.

7. Alés A. Study of different structures derives of β−Cu3Al by means of ab-initio calculations and quasi-harmonic approximation. *Computational Condensed Matter*, 2022, vol. 31, p. e00652. DOI: 10.1016/j.cocom.2022.e00652.

8. Hallstedt B., Gröbner J., Hampl M., Schmid-Fetzer R. Calorimetric measurements and assessment of the binary Cu-Si and ternary Al-Cu-Si phase diagrams. *Calphad*, 2016, vol. 53, pp. 25–38. DOI: 10.1016/j.calphad.2016.03.002.

9. Sufryd K., Ponweiser N., Riani P., Richter K.W., Cacciamani G. Exper-imental investigation of the Cu-Si phase diagram at x(Cu)>0.72. *Intermetallics*, 2011, vol. 19 (10), pp. 1479–1488. DOI: 10.1016/j.intermet.2011.05.017.

10. Phillips H.W.L. The constitution of aluminum-copper-silicon alloys. *Journal of the Institute of Metals*, 1953, vol. 82, pp. 9–15.

11. Raghavan V. Al-Cu-Si (Aluminum-Copper-Silicon). *Journal of Phase Equilibria and Diffusion*, 2007, vol. 28, pp. 180–182. DOI: 10.1007/s11669-007-9024-y.

12. He C.-Y., Du Y., Chen H.-L., Xu H. Experimental investigation and thermodynamic modeling of the Al-Cu-Si system. *Calphad*, 2009, vol. 33, pp. 200–210. DOI: 10.1016/j.calphad.2008.07.015.

13. Riani P., Sufryd K., Cacciamani G. About the Al-Cu-Si isothermal sec-tion at 500 °C and the stability of the ε-Cu15Si4 phase. *Intermetallics*, 2009, vol. 17, pp. 154–164. DOI: 10.1016/j.intermet.2008.10.011.

14. Miettinen J. Thermodynamic description of the Cu-Al-Si system in the copper-rich corner. *Calphad*, 2007, vol. 31, pp. 449–456. DOI: 10.1016/j.calphad.2007.05.001.

15. Ponweiser N., Richter K.W. New investigation of phase equilibria in the system Al-Cu-Si. Journal of *Alloys and Compounds*, 2012, vol. 512, pp. 252-263. DOI: 10.1016/j.jallcom.2011.09.076

16. Filippov A., Shamarin N., Moskvichev E., Savchenko N., Kolubaev E., Khoroshko E., Tarasov S. Heat input effect on microstructure and mechanical properties of Electron Beam Additive Manufactured (EBAM) Cu-7.5wt.%Al Bronze. *Materials*, 2021, vol. 14 (22), p. 6948. DOI: 10.3390/ma14226948.

17. Filippov A., Shamarin N., Moskvichev E., Savchenko N., Kolubaev E., Khoroshko E., Tarasov S. The effect of heat input, annealing, and deformation treatment on structure and mechanical properties of Electron Beam Additive Manufactured (EBAM) silicon bronze. *Materials*, 2022, vol. 15, p. 3209. DOI: 10.3390/ma15093209.

18. Zykova A., Panfilov A., Chumaevskii A., Vorontsov A., Gurianov D., Savchenko N., Kolubaev E., Tarasov S. Decomposition of β′-martensite in an-nealing the additively manufactured aluminum bronze. *Materials Letters*, 2023, vol. 338, p. 134064. DOI: 10.1016/j.matlet.2023.134064.

19. Shangina D.V., Gubicza J., Dodony E., Bochvar N.R., Straumal P.B., Tabachkova N.Yu., Dobatkin S.V. Improvement of strength and conductivity in Cu-alloys with the application of high pressure torsion and subsequent heat-treatments. *Journal of Materials Science*, 2014, vol. 49, pp. 6674–6681. DOI: 10.1007/s10853-014-8339-4.

20. Valiev R.Z., Islamgaliev R.K., Alexandrov I.V. Bulk nanostructured materials from severe plastic deformation. *Progress in Materials Science*, 2000, vol. 45, pp. 103–189. DOI: 10.1016/S0079-6425(99)00007-9.

21. *Filippov A.V., Khoroshko E.S., Shamarin N.N., Kolubaev E.A., Tarasov S.Yu.* Study of the properties of silicon bronze-based alloys printed using electron beam additive manufacturing technology. *Obrabotka metallov (tekhnologiya, oborudovanie, instrumenty) = Metal Working and Material Science*, 2023, vol. 25, no. 1, pp. 110–130. DOI: 10.17212/1994-6309-2023-25.1-110-130. (In Russian).

22. Besson R., Avettand-Fenoel M.-N., Thuinet L., Kwon J., Addad A., Roussel P., Legris A. Mechanisms of formation of Al4Cu9 during mechanical alloying: An experimental study. *Acta Materialia*, 2015, vol. 87, pp. 216–224. DOI: 10.1016/j.actamat.2014.12.050.

23. Faizova S.N., Aksenov D.A., Faizov I.A., Nazarov K.S. Unusual kinetics of strain-induced diffusional phase transformations in Cu-Cr-Zr alloy. *Letters on Materials*, 2021, vol. 11 (2), pp. 218–222. DOI: 10.22226/2410-3535-2021-2-218-222.

24. Tolmachev T.P., Pilyugin V.P., Patselov A.M., Gapontseva T.M., Plotnikov A.V., Churbaev R.V., Inozemtsev A.V. Features of the strain-induced dissolution and structure of fracture surfaces in Cu-Co alloys. *Diagnostics, Resource and Mechanics of Materials and Structures*, 2019, iss. 6, pp. 48–57. DOI: 10.17804/2410-9908.2019.6.048-057. (In Russian).

25. Ma S., Li X., Yang X., Fu L., Liu L., Xia M., Shan A. Effect of annealing temperature on microstructure and properties of a heavy warm rolled nickel aluminum bronze alloy. *Metallurgical and Materials Transactions A*, 2023, vol. 54, pp. 293–311. DOI: 10.1007/s11661-022-06873-1.

26. Naydenkin E.V., Grabovetskaya G.P. Deformation behavior and plastic strain localization of nanostructured materials produced by severe plastic deformation. *Materials Science Forum*, 2009, vol. 633–634, pp. 107–119. DOI: 10.4028/www.scientific.net/MSF.633-634.107.

27. Panin V.E., Egorushkin V.E., Panin A.V. Fizicheskaya mezomekhanika deformiruemogo tverdogo tela kak mnogourovnevoi sistemy. 1. Fizicheskie osnovy mnogourovnevogo podkhoda [Physical Mesomechanics of Deformable Solids as a Multilevel System. I. Physical Fundamentals of the Multilevel Approach]. *Fizicheskaya mezomekhanika = Physical Mesomechanics*, 2006, vol. 9, no. 3, pp. 9–22. (In Russian).

28. Grabovetskaya G.P., Mishin I.P., Kolobov Yu.R. Vliyanie dispersnogo uprochneniya na zakonomernosti i mekhanizmy polzuchesti medi s submikrometrovym razmerom zeren [The effect of precipitating hardening on regularities and mechanisms of submicron-grain copper creep]. *Izvestiya vysshikh uchebnykh zavedenii. Poroshkovaya metallurgiya i funktsional'nye pokrytiya = Powder Metallurgy and Functional Coatings*, 2009, no. 2, pp. 38–43. (In Russian).

29. Kozlov E.V., Zhdanov A.N., Koneva N.A. Bar'ernoe tormozhenie dislokatsii. Problema Kholla-Petcha [Barrier hindrance of dislocations. The Hall-Petch problem]. *Fizicheskaya mezomekhanika = Physical Mesome-chanics*, 2006, vol. 9, no. 3, pp. 81–92. (In Russian).

30. Faizov I.A., Mulyukov R.R., Aksenov D.A., Faizova S.N., Zemlyakova N.V., Cardoso K., Zeng Y. Rastvorenie chastits vtorykh faz v nizkolegirovannom mednom splave sistemy Cu-Cr-Zr pri obrabotke metodom ravnokanal'nogo uglovogo pressovaniya [Dissolution of second-phase particles in a low-alloyed copper alloy of the Cu-Cr-Zr system processed by equal-channel angular pressing]. *Pis'ma o materialakh = Letters on Materials*, 2018, vol. 8, no. 1, pp. 110–114. DOI: 10.22226/2410-3535-2018-1-110-114. (In Russian).

31. Ilie F. Tribological behaviour of the steel/bronze friction pair (journal bearing type) functioning with selective mass transfer. *International Journal of Heat and Mass Transfer*, 2018, vol. 124, pp. 655–662. DOI: 10.1016/j.ijheatmasstransfer.2018.03.107.

Conflicts of Interest

The authors declare no conflict of interest.